

INFLUENCE OF DISPERSIVE Y_2O_3 PARTICLES ALLOYING BY LASER IRRADIATION ON OXIDATION BEHAVIOUR OF AN SUPERALLOY^①

Xu, Wanren Meng, Qinglin Zou, Yuchao

Northeastern University, Shenyang 110006, China

ABSTRACT

The homogeneous dispersive Y_2O_3 particles were melt-doped on the surface of a superalloy by laser alloying and the effect of Y_2O_3 on the oxidation resistance of the alloy were investigated. The results showed that compact α - Al_2O_3 oxide scales formed continuously on the alloy surface and the internal oxidation was eliminated and oxidation rate decreased. Therefore, the oxidation resistance of the alloy was improved.

Key words: superalloy Y_2O_3 particle laser surface alloying oxidation resistance

1 INTRODUCTION

Rare earth elements and their oxides particles may improve prominently high temperature oxidation and corrosion resistance of materials^[1-3]. At present, various protective coatings are used to modify the oxidation and corrosion behaviour of superalloys and the MCrAlY (here, M represents metallic elements) coatings are superior and investigated more. The oxide Y_2O_3 particles dispersion strengthening ODS alloy has both higher temperature strength and high temperature oxidation corrosion performance. The laser surface alloying was tried to dope the Y_2O_3 particles on the surface of the superalloy and the ODS alloy layer obtained in this paper and a new approach to the comprehensive strengthening for the superalloy surface is presented.

2 EXPERIMENTAL METHOD

The composition of γ' phase precipitation strengthening GH49 superalloy selected

as substrate material is the Ni-10Cr-15Co-5.5W-5Mo-4Al-1.6Ti-0.3V (wt.-%) and used at temperatures of 850~900 °C. The specimens ($26 \text{ mm} \times 6 \text{ mm}$) was cut from hot rod. The Y_2O_3 particles of mean size 0.05 μm were obtained and the alloy surface precoated by 0.05 g/cm^2 Y_2O_3 powder was irradiated by continuous CO_2 laser beam with Ar atmosphere. The laser power density was $1.76 \times 10^4 \text{ W}/\text{cm}^2$, the scanning speed is 0.36 m/min. The heat treatment is 1200 °C, 2 h, air cool + 1050 °C, 4 h, air cool + 850 °C, 8 h, air cool after laser irradiation. The specimens GH49 of undoped Y_2O_3 and doped Y_2O_3 were then oxidized at 950 °C for 100 h in air. Following these, the morphology of the specimens after laser irradiation and oxidation were observed by optical microscope and the scanning electron microscope (SEM). The distribution of Y_2O_3 particles was analyzed by electronic probe microanalyzer (EPMA) and the surface phase composition of the oxidized specimens was determined

① Financially supported by the Ministry of Metallurgical Industry; manuscript received Dec. 15, 1992

with X-ray diffractometer (XRD).

3 EXPERIMENTAL RESULTS AND DISCUSSION

3.1 Microstructure of Laser Alloying Layer and Y_2O_3 Particles Distribution

Fig. 1 (a) shows dendritic microstructure in melted zone after laser treatment. The dendritic grains grow preferentially to the surface at the boundary of melted zone and heat affected region. In order to achieve dispersion strengthening, 0.5~2.0 wt.-% content of Y_2O_3 is required and distributed homogeneously. The yttrium and oxygen elements analyzed by EPMA showed the fluctuation curves for both elements and have corresponding distribution. It indicates that the Y_2O_3 powder didn't change after laser irradiation. Therefore, the distribution of Yttrium represents that of Y_2O_3 particles. Fig. 1 (b) shows the micro-distribution of Y element on the cross section of laser melted region. One can see that the Y_2O_3 particles exist in the alloyed region and they distribute homogeneously from surface to the boundary of the melted zone. Combined with the homogeneous linear distribution of Y_2O_3 ^[4], it can be deduced that the Y_2O_3 particles are in the whole melted zone. By measurement, the alloying zone

has a width of 3.6 mm and a depth of 1.2 mm and the content of Y_2O_3 is about 1.2 wt.-%~1.5 wt.-%, the ODS alloying achieved.

Fig. 2 shows the micrographs of alloying zone after heat treatment. It can be seen that the dendritic structures disappeared and the fine grains, the curved boundary, the γ' phases and carbides were observed. Therefore, alloying layer containing γ' phase and Y_2O_3 particles were formed on the alloy surface which is similar to the ODS alloy structure.

3.2 Oxidation Behaviour of laser Alloying layer

(1) Oxidation kinetics

Fig. 3 shows the oxidation curves of the laser melt-doped Y_2O_3 and undoped Y_2O_3 specimens after oxidation at 950 °C. It can be observed that the gained weight of doped Y_2O_3 specimen is less than that of undoped Y_2O_3 alloy, and with increasing oxidation time the difference in weight of these two samples increases. That is the reason for increase in resistance to oxidation of the alloy.

(2) Micrographs and microanalysis on Cross-sections

After 100 h oxidation, it could be observed that the surface oxide scales of undoped

Fig. 1 Microstructure and micro-distribution of Y on the cross section of laser alloying region
(a)—microstructure; (b)—micro distribution of Y

Fig. 2 Structure of laser alloying layer and substrate material after heat treatment
(a)—laser alloying layer ($\times 100$); (b)—substrate material ($\times 125$)

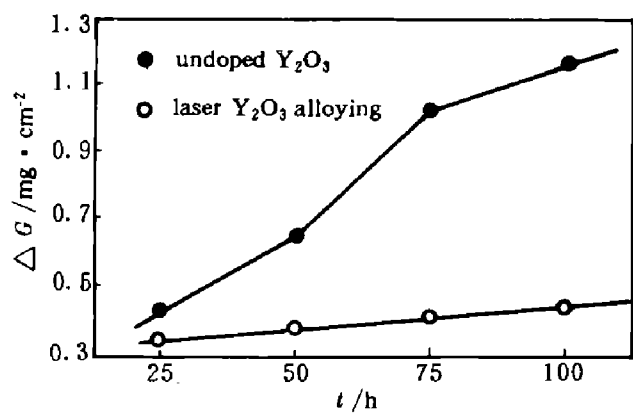


Fig. 3 Oxidation kinetics curves of the alloys of melt-doped Y_2O_3 and undoped Y_2O_3

ped Y_2O_3 specimen were deeper than that of the doped Y_2O_3 specimen and spalled heavily. Fig. 4 and Fig. 5 show that the second electron and X-ray images for undoped and doped Y_2O_3 alloys after 100 h oxidation respectively. The micrograph of cross section in Fig. 4 showed the external, internal oxide layer, poor element region and the matrix. However, in Fig. 5, no external oxide scale and internal oxides were observed from the doped Y_2O_3 specimen. With XRD, the external oxide scales of both specimens were complex oxides including Cr_2O_3 , α - Al_2O_3 , NiCr_2O_4 , CoCr_2O_4 etc, but less oxides were obtained for the doped Y_2O_3 specimen. From Figs 4 and 5, we can find that thick loose

and uncontinuous Cr_2O_3 oxide scale formed on the surface of undoped Y_2O_3 specimen and internal Al_2O_3 oxide formed under surface scales, the internal oxide layer and poor element region become wide ($43 \mu\text{m}$). However, a thin continuous compact Al_2O_3 scale formed on the surface of doped Y_2O_3 specimen and no oxides obtained under the surface. The whole poor element layer was very thin, about $1/7$ the undoped Y_2O_3 specimen.

Generally, the effect of Y_2O_3 is considered similar to Y , or even better than Y ^[5]. Li, *et al*^[6] studied the influence of Y_2O_3 particles on the oxidation resistance behaviour of β - NiAl coating on the surface of cast Ni-based superalloy M38 and pointed out that Y_2O_3 promotes the formation of oxidate layer, and improves its quality and reduces its oxidation rate and increases its adhesion by pinning effect. Sohan *et al*^[7] and Hong Yongjing^[8] studied the oxidation behaviour of Y_2O_3 -added 316L stainless steel and Ni-20Cr alloy and also obtained the similar conclusion. According to this experimental result, the role of Y_2O_3 particle to improve the oxidation resistance of the superalloy is due to the fact that it decreases oxidation reaction area, by addition of Y_2O_3 particles, the

Fig. 4 Second electron and X-ray images of unmelt-doped Y_2O_3 alloy after oxidation for 100 h at 950 $^{\circ}\text{C}$ ($\times 1500$)
(a)—second electron image; (b)—Cr; (c)—Al; (d)—Ni

weight gain and the oxidation rate reduced. Y_2O_3 reduced the Al content needed for Al_2O_3 and promoted the selective oxidation of Al element in alloy; fine grained microstructure formed laser rapid melt-solidification may act as paths for short distance diffusion of Al element and speed up the external oxidation of Al. Therefore, the Cr_2O_3 scale of the alloy changes into Al_2O_3 scale with better high temperature oxidation resistance. The Y_2O_3 particles acting as sites for inhomogeneous nucleation of α - Al_2O_3 scales and grains of oxides are very smaller, the continuous compact protective oxides scales were formed. Moreover, the Y_2O_3 modified the adhesion of scale and the scales became uneasy to crack and spall. So the protective Al_2O_3 scale can effectively hinder the oxygen

diffusion from dispersing to matrix during its oxidation and diffusion of Cr, Al etc from the substrate to the surface, dispel the internal oxidation and decrease the growth rate of the oxide layers and the element lacking layer and thus resulting the oxidation rate to be reduced. While for undoped Y_2O_3 specimen, because of its high content of Cr element in the alloy the Cr_2O_3 scale formed first on the surface of the alloy during oxidation. This oxide scale is worse than Al_2O_3 scale in oxidation resistance, since it is uncontinuous and has loose structure, under a conditions of alternative hot-cool changes the oxide scale is easy to induce concentration of thermal stresses and thus leading the scale to crack and spall and the oxidation rate of alloy be increased rapidly.

Fig. 5 Second electron and X-ray images of Y_2O_3 alloying ($\times 1500$)
specimen after oxidation for 100 h at 950 °C
(a)—second electron image; (b)—Al; (c)—Cr; (d)—Ni

Concerning the microstructure and performance of the laser surface Y_2O_3 alloying layer, it is considered to be a new and fine surface protective layer of the superalloy.

4 CONCLUSIONS

(1) The dispersive and homogeneous Y_2O_3 particles can be doped on the surface of the superalloy by laser alloying and formed oxides dispersion strengthening layer similar to the ODS alloy.

(2) The addition of Y_2O_3 particles can promote the formation of the continuous compact protective α - Al_2O_3 oxides scales and modify its adhesion of the scale. Therefore,

the oxidation rate of the alloy was reduced and the oxidation resistance of the superalloy was greatly improved.

REFERENCES

- 1 Ramanarayanan, T A *et al.* *Oxid Met*, 1984, 22: 83.
- 2 Glasgow, T K *et al.* *Oxid Met*, 1981, 15: 95.
- 3 Yin, Y D *et al.* *J of Corrosion and Protection of Society of China*, 1982, 2: 35.
- 4 Meng, Q L *et al.* *Chin J Met Sci Technol*, 1992, 8: 343.
- 5 The Application of Rare Earth in Iron and Steel. Beijing: Metallurgical industry press, 1987. 313.
- 6 Li, T F *et al.* *J of the Chinese Rare Earth Society*, 1991, 9: 229.
- 7 Sohan, L *et al.* *Oxid Met*, 1989, 32: 317.
- 8 Hong, Yongjing *et al.* *Foreign Metal Materials*, 1983, 10: 54.